NUMERICAL SIMULATION OF GAS-SOLID FLOW IN THE RISER OF CIRCULATING FLUIDIZED BEDS – A TURBULENCE ANALYSIS APPROACH

Luben Cabezas Gómez
Núcleo de Engenharia Térmica e Fluidos - NETeF, EESC/USP. Av. Trabalhador São-carlense, 400, Centro, São Carlos - SP, CEP 13566-590.
e-mail: lubencg@sc.usp.br

Fernando Eduardo Milioli
Núcleo de Engenharia Térmica e Fluidos - NETeF, EESC/USP. Av. Trabalhador São-carlense, 400, Centro, São Carlos - SP, CEP 13566-590.
e-mail: milioli@sc.usp.br

Abstract. Turbulence parameters are derived from results of numerical simulation of gas-solid flow in circulating fluidized beds (CFB). A two fluids model with constant viscosity is applied considering an Eulerian approach for both phases. Reynolds stresses and granular temperature are derived from numerical data. An analysis is performed assuming that a direct numerical simulation (DNS) has actually been carried out for the solid phase. This seams to be reasonable since the applied computational mesh size is very large as compared to the mean free path among the solid particles. Even though velocity fluctuations of lower scales are eliminated, fluctuations of larger scales are detected and analyzed. Of course, as far as the gas phase is concerned the mesh is very coarse, and no DNS is applied. The results show that the Reynolds stresses behave according to the expected for a turbulent flow, and a good agreement is found regarding literature experiment. Also, following the literature, granular temperature is derived from the Reynolds stresses, and qualitatively match the expected behavior as described by the kinetic theory of granular flow (KTGF).

Keywords. Numerical simulation, Gas-solid flow, Riser, Circulating fluidized beds, Turbulence

1. Introduction

Turbulence modeling of multiphase flows is quite complex. In addition to the formulation difficulties found in single-phase flows, in multiphase fluids the interface interactions must be described. When the interface is well defined, as in gas-liquid stratified flows, a more rigorous modeling approach can be performed. In gas-solid and other multiphase non-stratified flows, where the interface is not well defined, modeling is much less straightforward.

In order to recover scales of turbulent fluctuations which are lost in view of numerical mesh scales, models need to artificially incorporate them into the conservative balance equations. Besides, interface interactive terms must be formulated so that the turbulence of a phase is allowed to affect the other phase and vice-versa. Concerning artificially introduced fluctuations, a number of procedures are available for single-phase flows. Those procedures are also applied to multiphase flows, even though modified so that the multiphase physics can be better approached.

Interface interactive parameters have been derived from the so called kinetic theory of granular flow (KTGF), which is an analogy with the kinetic theory of dense gases (Chapman & Cowling, 1970). Parameters analogous to thermodynamic and physic properties have been derived for the solid phase, such as granular temperature and solid phase viscosity. Newtonian rheology has been applied to both phases, and turbulence has been accounted for through artificial procedures like the well known k-ε model (Peirano & Leckner, 1998).

Many authors consider the KTGF to account for the turbulence of the solid phase in a similar way as the k-ε model does (Peirano & Leckner, 1998, and Gidaspow, 1994, among others). However, as pointed by Sinclair (1997), this is still a very open question. Sinclair notes that granular temperature is related to velocity fluctuations of individual particles, while the velocity fluctuations of collections of particles relate to turbulent kinetic energy. The concepts are quite distinct and should not be mixed up. It is not possible to determine the thermodynamic temperature from macroscopic continuum hydrodynamic predictions. The same way, it is not fair to determine granular temperature from the mean motion of collections of particles (a continuum defining the solid phase). Granular temperature should be determined either from velocity fluctuations of particles, or by solving a conservative equation for granular energy.

In this work the turbulence of the solid phase is approached through direct numerical simulation (DNS) commonly applied in single-phase turbulence analysis. The principle is that, if a computational mesh is sufficiently fine, all hydrodynamic phenomena of a continuum flow field can be resolved through the conventional Navier-Stokes equations. A not fine enough mesh size shall filter turbulent scales of higher frequencies. A relatively coarser mesh shall allow detection of turbulent scales only at lower frequency levels. By applying a DNS approach to the solid phase for a given mesh size, fluctuations of higher frequencies are filtered. However, fluctuations of lower frequencies characterizing large scales of turbulence imposed for instance by geometry, can be predicted. Thereby it is possible to state that at least the large scale turbulence can be predicted by the usual two fluids models, and no additional procedure is required to deal with turbulence. The way by which the larger scales depend upon smaller scales, and vice-versa, is quite unknown and is a matter for further research. Sundaresan (2000) observes that this relationship mechanism is apparently much different as compared to that observed in turbulent single-phase flows.

Both time and apace mesh scales can be further refined regarding those applied in this work. However, caution is required not to undertake the minimum limit on spatial mesh size having in view the validity of the average Eulerian

continuum equations for the solid phase. It is not possible to refine the mesh beyond that limit and still mantain the validity of a continuum formulation. Either, for gas and particulate, the limit is of about one order of magnitude above the mean free path among molecules or particles. The limit for the particulate results several orders higher than that for the gas phase. The limit for the gas phase is much lower than that required for catching the smallest turbulent structures, which is about one order above the mean free path among the Kolmogorov dissipative scales.

In this work Reynolds stresses and granular temperature are derived from numerical data. It has been pointed out above that granular temperature should not be determined through continuum hydrodynamic data. In spite of that this is done in this work for two reasons. First, to follow a literature common tendency in view of favorable comparison to experiment (Matonis et al., 2002). Second, to generated data for further checking against possible new experiment. Following Peirano & Leckner (1998) and Matonis et al. (2002), granular temperature is assumed equal to two thirds of the turbulent kinetic energy.

2. Formulation

2.1 Mathematical model

The simulations presented in this work are generated through the hydrodynamic model B developed at IIT (Illinois Institute of Technology) by D. Gidaspow and co-workers. In particular, the MICEFLOW code (Jayaswal, 1991) is utilized. A summary of the governing equations is presented in Table 1. More detailed descriptions can be found in Jayaswal (1991), Gidaspow (1994), Enwald et al. (1996) and Cabezas-Gómez & Milioli (2001). The model, generally known as traditional two fluids model, is based on a continuum Eulerian description for each phase. More recently, it has been enhanced by the introduction of the kinetic theory of granular flow (KTGF) (see for instance Gidaspow, 1994).

The general model accounts for conservation of mass, momentum and energy for all the phases, and turbulent kinetic energy for solid phases. The computational code allows the description of multiphase flows including two different fluid phases, and several different solid phases, each one characterized by averages of particle diameter, density and shape factor. In this work a gas-solid flow is considered comprising one gas phase (air) and one solid phase (glass balls). Newtonian rheology is assumed. Only mass and momentum conservative equations are solved for both phases in two-dimensional flows, and no interface mass transfer is considered. The pressure of the solid phase is modeled by applying the concept of solid's phase elasticity module through the correlation of Rietema & Mutsers (Rietema & Mutsers, 1973, apud Jayaswal, 1991). The interface drag function is modeled through a literature commonly used procedure (Gidaspow, 1994), using Ergun's correlation (Ergun, 1952) when solid's fraction is equal or higher than 0.2, and Wen and Yu's correlation (Wen & Yu, 1966) when solid's fraction is lower than 0.2.

2.2 Derivation of turbulent and flow parameters

Reynolds stresses are defined by products of time averaged velocity fluctuations (Tennekes & Lumley, 1977). For both phases, normal and shear Reynolds stresses are determined by the following (Mudde et al., 1997, Pan et al., 2000, Matonis et al., 2002)

$$\left\langle u_k^{'} u_k^{'} \right\rangle = \frac{1}{N} \sum_{n=1}^{N} u_k u_k - \overline{u}_k^2 \tag{1}$$

$$\left\langle v_k^{'} v_k^{'} \right\rangle = \frac{1}{N} \sum_{n=1}^{N} v_k v_k - \overline{v}_k^2 \tag{2}$$

$$\left\langle u_k^{'} v_k^{'} \right\rangle = \frac{1}{N} \sum_{n=1}^{N} \left[(u_k - \overline{u}_k)(v_k - \overline{v}_k) \right] \tag{3}$$

where N represents the number of vectors considered in the time averaged calculations. The considered time interval was 80 seconds of real flow, with a numerical time steps of 0.01 seconds, resulting N equals to 8000 vectors. The time interval was counted from 20 to 100 seconds, since a statistically developed regime was identified starting at about 20 seconds of real flow.

The solid phase granular temperature was determined as a function of the turbulent kinetic energy by the following (Peirano & Leckner, 1998, Matonis et al., 2002)

$$\theta_s = \frac{1}{3} \left(< u_s^{'} u_s^{'} > + < v_s^{'} v_s^{'} > \right) = \frac{2}{3} k_s \tag{4}$$

where k_s is the turbulent kinetic energy by unit of mass of the solid phase (m^2/s^2).

The dynamic viscosity of the solid phase is determined as a function of the granular temperature by the following (Gidaspow, 1994)

$$\mu_s = \frac{5\rho_s d_p \sqrt{\pi\theta_s}}{48(1+e)g_0}\left[1+\frac{4}{5}(1+e)g_0\alpha_s\right]^2 + \frac{4}{5}\alpha_s^2\rho_s d_p g_0(1+e)\sqrt{\frac{\theta_s}{\pi}} \tag{5}$$

where g_0 is a radial distribution function associated to particles, determined from Bagnold's correlation (Bagnold, 1954); and **e** is the restitution coefficient between particles of the solid phase, assumed equal to 0.995 (Gidaspow, 1994).

Table 1: Mathematical Model B (Gidaspow, 1994).

1. Continuity, phase k (k = g, s)

$$\frac{\partial(\rho_k\alpha_k)}{\partial t} + \nabla\cdot(\rho_k\alpha_k\mathbf{v}_k) = 0$$

2. Momentum, Model B

Gas phase:
$$\frac{\partial(\rho_g\alpha_g\mathbf{v}_g)}{\partial t} + \nabla\cdot(\rho_g\alpha_g\mathbf{v}_g\mathbf{v}_g) = -\nabla P$$
$$-\beta_B(\mathbf{v}_g - \mathbf{v}_s) + \nabla\cdot(\alpha_g\tau_g) + \rho_g\mathbf{g}$$

Solid phase:
$$\frac{\partial(\rho_s\alpha_s\mathbf{v}_s)}{\partial t} + \nabla\cdot(\rho_s\alpha_s\mathbf{v}_s\mathbf{v}_s) = \beta_B(\mathbf{v}_g - \mathbf{v}_s)$$
$$+ \nabla\cdot(\alpha_s\tau_s) - G\nabla\alpha_s + (\rho_s - \rho_g)\alpha_s\mathbf{g}$$

3. Viscous stress tensor, phase k (k = g, s)

$$\tau_k = \mu_k\left[\nabla\mathbf{v}_k + (\nabla\mathbf{v}_k)^T - \frac{2}{3}(\nabla\cdot\mathbf{v}_k)I\right]$$

4. Solid elasticity modulus

$$G(\alpha_g) = 10^{-8.686\alpha_g+6.385} \quad \text{dyn}/\text{cm}^2$$

5. Volumetric fraction

$$\alpha_g + \alpha_s = 1$$

Simbology

C_{Ds} – drag coefficient for a single particle in an Infinite medium
d_p – particle diameter, (m)
g – gravity acceleration, (m/s^2)
G – solid elasticity modulus (N/m^2)
P – gas pressure (Pa)
Re_s - Reynolds number based on particle diameter
R_g – ideal gas constant, (kJ/kgK)
t – time, (s).
$\mathbf{v}_g$ and $\mathbf{v}_s$ – average velocities, (m/s)

6. Gas law

$$\rho_g = P/(R_g T)$$
$$\rho_s = \rho_s \text{ (constant)}$$

7. Interface drag function, Model B

Ergun (1952) for $\alpha_s \geq 0.2$:
$$\beta = 150\frac{\alpha_s^2\mu_g}{\alpha_g^2(d_p\phi_s)^2} + 1.75\frac{\rho_g\alpha_s|\mathbf{v}_g - \mathbf{v}_s|}{(\alpha_g d_p\phi_s)}$$

Wen & Yu (1966) for $\alpha_s < 0.2$:
$$\beta = \frac{3}{4}C_{Ds}\frac{\rho_g\alpha_s\alpha_g|\mathbf{v}_g - \mathbf{v}_s|}{(\alpha_g d_p\phi_s)}\alpha_g^{-2.65}$$

where
$$C_{Ds} = \begin{cases} \dfrac{24}{Re_s}(1+0.15\cdot Re_s^{0.687}) & Re_s < 1000 \\ 0.44 & Re_s \geq 1000 \end{cases}$$

Reynolds number
$$Re_s = \frac{\alpha_g\rho_g|\mathbf{v}_g - \mathbf{v}_s|d_p\phi_s}{\mu_g}$$

β – interface drag function, (kg/m^{2}s)
μ – dynamic viscosity, (kg/ms)
α_g and α_s – volumetric fractions
ρ_g and ρ_s – densities, (kg/m^3)
τ_g and τ_s – viscous stress tensors, (Pa)
ϕ_s – particle sphericity

Subscripts

(g) and (s) – gas and solid phases

3. Geometry, initial and boundary conditions

Figure 1 shows the geometry and domain considered in the simulation. The initial and boundary conditions at entrance and exit for both phases are also presented. At entrance a one-dimensional plug flow is considered. At exit the continuity condition is applied to all variables. At the walls a non-slip condition is assumed for the gas phase, while a partial slip condition is applied for the solid phase following Ding & Gidaspow (1990). A cartesian numerical mesh 22x297 was applied which is uniform by blocks in the axial direction as shown in Figure 1. A constant solid phase viscosity was considered which was obtained from experiment by Tsuo & Gidaspow (1990).
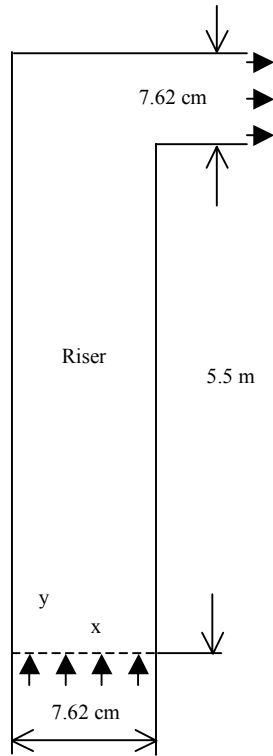
Simulation data:
Particles diameter: $d_p = 520 \ \mu m$
Particle density: $\rho_s = 2620 kg/m^3$
Solid phase mass velocity: $G_s = 24,9 \ kg/(m^2s)$
Gas phase viscosity: $\mu_g = 1,8 \times 10^{-5} \ Pa \ s$
Solid phase viscosity: $\mu_s = 0,509 \ Pa \ s$
Initial conditions:
Riser without solid
$P = 101,325 \ kPa$
$T = 300 \ K$
Entrance boundary conditions:
$v_s = 0,386 \ m/s$
$v_g = 4,979 \ m/s$
$\alpha_s = 0,0246$
$P = 121,590 \ kPa$
$T = 300 \ K$
Exit boundary condidions:
Continuity condition

$$\frac{\partial f}{\partial x} = 0 \qquad (6)$$

for $f = \alpha_g, \ u_g$ or u_s
Gas phase pressure: $P = 117,2049 \ kPa$
Computational conditions:
$\delta x = 22 \times 0,381 \ cm$
$\delta y_1 = 11 \times 1,66; \ \delta y_2 = 280 \times 1,905; \ \delta y_3 = 6 \times 1,524 \ (cm)$
$\delta t = 0,00005 \ s$
Number of cells: $(22 \times 297) = 6534$
Real time of simulation: $t = 100 \ s$

Figure 1. 2D geometry and domain, initial and boundary conditions, and computational conditions for the simulations of the IIT installation (Luo, 1987; Tsuo & Gidaspow, 1990).

4. Results

Firstly, simulated radial profiles of solid fraction and axial velocities for both phases are compared to experimental data. Then, results of Reynolds stresses are presented and discussed. Owing to the lack of experimental data on CFB, the predicted Reynolds stresses are qualitatively compared to literature predictions and experiment in gas-liquid and gas-liquid-solid flows. Finally, the predicted granular temperature and solid viscosity are compared to literature data derived from predictions and experiment in CFB.

Figure 2 presents time averaged radial profiles of axial velocity for both phases compared to the experimental data of Luo (1987). For the gas phase the relative deviations are quite significant, mainly at the axis. This may be a consequence of not accounting for the gas phase turbulence in the model. Experimental uncertainties on gas phase local velocities measurement may also significantly contribute to the deviations. The predicted solid phase axial velocity profile shows a much better behavior. The better predictions of velocity profiles of the solid phase related to the gas phase is further exploited in Cabezas-Gómez & Milioli (2002).

Figure 3a shows time averaged radial profiles of radial velocity for both phases. The profiles are almost inversely symmetric around the axis, and show the tendency for particle migration towards the walls. Figure 2 shows an annular layer of solid of negative axial velocity along the walls. The velocity profiles unveil the annular plug flow pattern and the segregation of solids towards the walls typical of CFBs. This fact is confirmed by the radial profile of solid fraction presented in Figure 3b, and by the instantaneous sketches of solid fraction along the column presented in Figure 4. The concentration of solids at the walls is also a cause for clustering, as observed in Figure 4 at the column left wall.

The computational mesh 22x297 used in this work is much finer than the 12x75 mesh used in a previous work for the same conditions (Cabezas-Gómez & Milioli, 2002). Despite quantitative differences, the results obtained with the two meshes are qualitatively similar. This shows that mesh size has no effect on predictions behavior, at least for the cases considered.
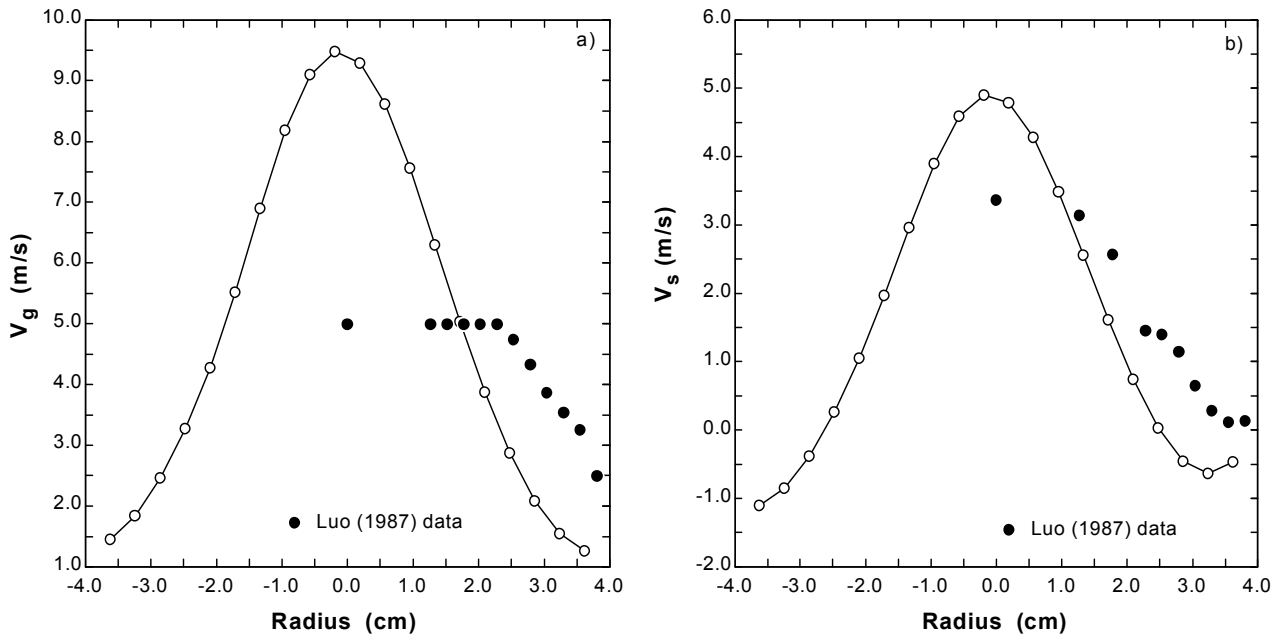
Figure 2. Time averaged radial profiles of axial velocity for both phases 3.4 m above entrance compared to the experimental data of Luo (1987). Time average from 20 to 100 s.
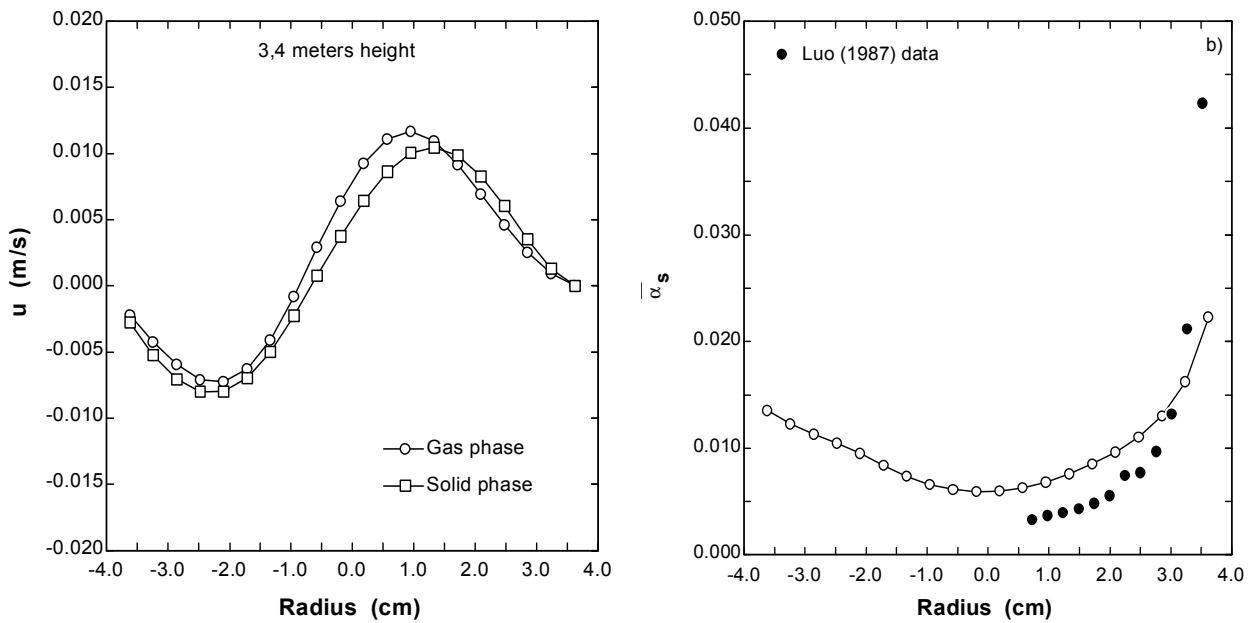

Figure 3. Time averaged radial profiles of radial velocity for both phases and solid fraction 3.4 m above entrance compared to the experimental data of Luo (1987). Time average from 20 to 100 s.

Figures 5 and 6 show radial profiles of normal and shear Reynolds stresses in various different sections of the column. Normal stresses result mostly symmetric and one-modal. Shear stresses result mostly inversely symmetric and two-modal. This behavior is in agreement with observations for gas-liquid columns of bubbles (Mudde et al., 1997, e Pan et al., 2000). The normal axial stresses $<v'v'>$ are superior by three orders of magnitude as compared to the normal radial stresses $<u'u'>$, and by two orders of magnitude as compared to the shear stresses $<u'v'>$. This is in disagreement with the results for both gas-liquid bubble columns of Mudde et al. (1997) and gas-liquid-solid bubble columns of Matonis et al. (2002). In those cases normal radial and axial stresses are of the same order, and are one order higher than the shear stresses. However, despite the disagreement regarding order of magnitude, the qualitative behavior of $<u_s'u_s'>$ and $<u_s'v_s'>$ is similar to that of the gas-liquid and gas-liquid-solid systems. The normal stresses $<u_s'u_s'>$ in the bubble columns are maximum close to the axis, since radial velocities are maximum at this region owing to a spinning motion of bubble streams. Supposingly, the up flow around the axis is quite uniform and consequently characterized by low fluctuations of radial velocity (Mudde et al., 1997). For the concerning gas-solid flow the profiles of axial and radial velocities cause segregation of solids at the walls and impose higher normal radial stresses around the axis.
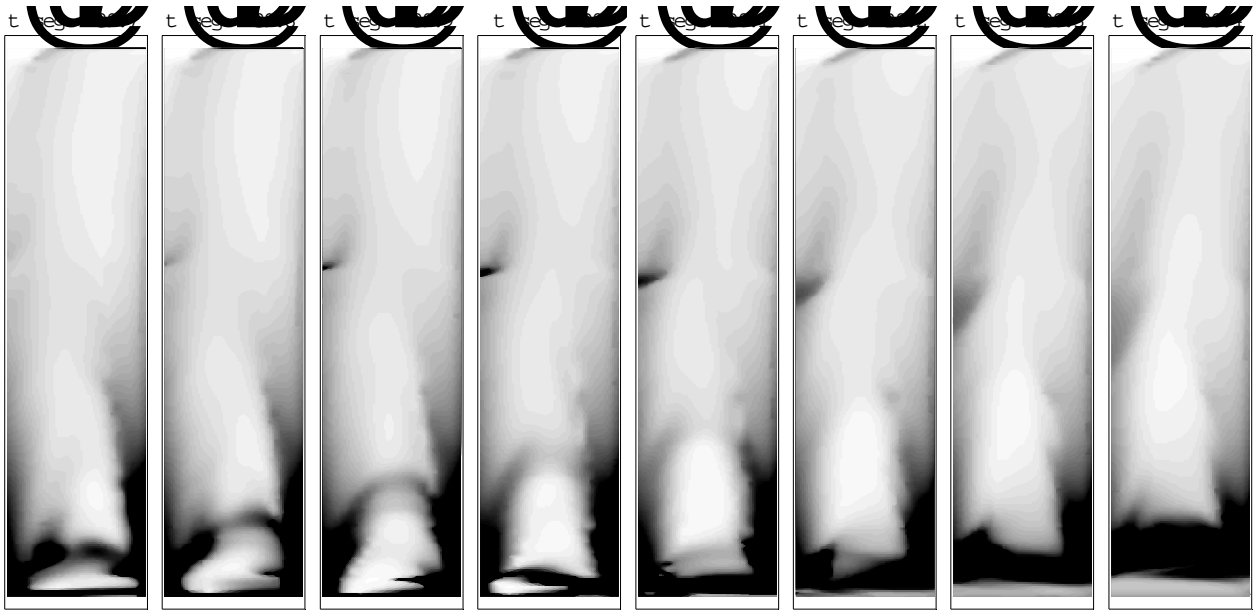
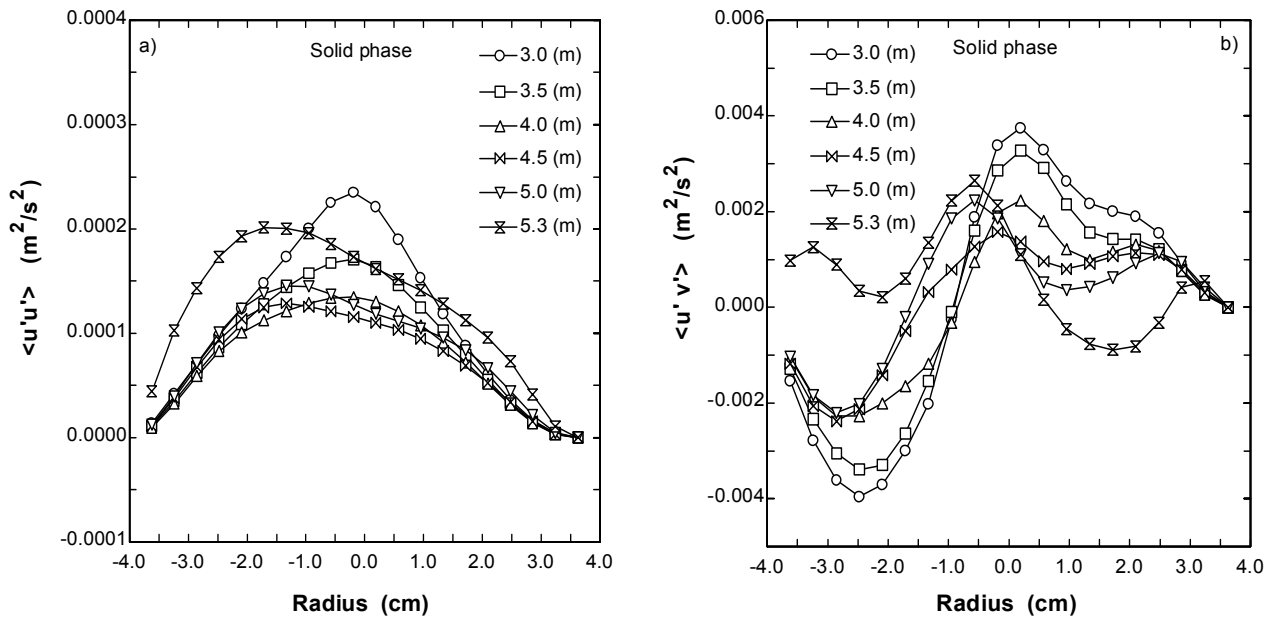Figure 4. Instantaneous sketches of solid fraction along the column.

Figure 5. Radial profiles of normal $\langle u_s'u_s'\rangle$ and shear $\langle u_s'v_s'\rangle$ Reynolds stresses in various different sections of the column.

The shear stresses for the concerning gas-solid flow behaves similarly to that of bubble flows. Besides, just like in the bubble columns, the shear stresses for the gas-solid flow tend to zero in regions close to the walls. The major qualitative differences between the considered cases relate to the $\langle v_s'v_s'\rangle$ profiles. While in the bubble columns of Mudde et al. (1997), Pan et al. (2000) and Matonis et al. (2002) a maximum appears close to the walls, in the concerning gas-solid flow a maximum is observed at the axis. In fact this behavior is typical of the $\langle u_s'u_s'\rangle$ profiles observed in the bubble columns. Mudde et al. and Matonis et al. attribute the behavior of the bubbly flows to the development of eddies with scales close to the diameter of the column, while according to Pan et al. it is due to the occurrence of a liquid downflow close to the walls.
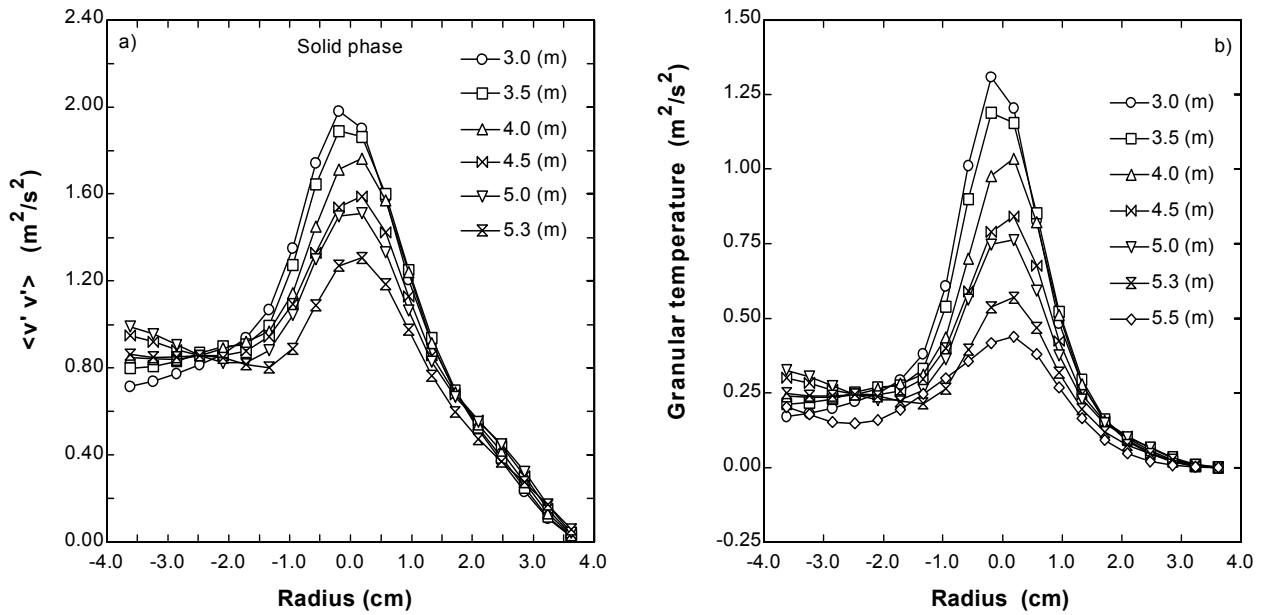
Figure 6. Radial profiles of normal $<v_s'v_s'>$ Reynolds stresses and granular temperature in various different sections of the column.

In the gas-solid flow, despite the existence of an annular downflow of solids at the walls and a diluted upflow plug around the axis, the normal stresses do not behave like in bubble columns. Despite the mismatching regarding bubble columns, there are evidences supporting the current predictions for gas-solid flow. Table 2 reproduces experimental data on granular temperature obtained by Gidaspow & Huilin (1998). The table shows that the axial component of the instantaneous particle velocity σ_z is up to two orders of magnitude higher than the radial component σ_θ, meaning that the normal axial stresses $<v_s'v_s'>$ in fact determine granular temperature. Such is clearly seen in Figure 6, where the profiles of granular temperature result very similar to the profiles of $<v_s'v_s'>$. The above allows to conclude that the differences in magnitude of $<v_s'v_s'>$ regarding both $<u_s'u_s'>$ and $<u_s'v_s'>$, are qualitatively correct.

Table 2: Measurements on granular temperature (Gidaspow & Huilin, 1998).

Runs	U_g (m/s)	G_s (kg/m^{2}s)	α_s	U_{av} (cm/s)	σ_θ (cm/s)	σ_z (cm/s)	θ_s (m^2/s^2)
1	2,89	19,03	0,0284	-18,20	19,45	198,29	1,33
2	2,89	20,89	0,0383	-31,26	15,83	213,36	1,54
3	2,89	24,33	0,0521	-52,53	23,33	258,74	2,27
4	2,89	4,380	0,0042	274,04	6,773	61,750	0,13
5	2,35	29,35	0,0924	-69,35	16,19	311,89	3,26
6	2,35	9,704	0,0025	235,35	11,49	75,928	0,21
7	2,35	20,36	0,0470	-31,02	32,78	222,22	1,72
8	2,35	29,57	0,0855	-76,02	21,08	285,38	2,74

θ_s – granular temperature = $(2/3)\sigma_\theta^2 + (1/3)\sigma_z^2$; U_g – gás superficial velocity; U_{av} – average particle velocity; σ_θ and σ_z – components of the instantaneous particle velocities along θ and z; α_s – solid fraction; G_S – solid mass velocity.

Figure 7 shows time averaged radial profiles of granular temperature and solid fraction in the column's left side. Granular temperature results maximum at the axis, where the solid fraction is minimum as expected from Gidaspow's results (Gidaspow, 2000). At the central core the flow is diluted, and the mean free path between particles results high. As a consequence, the fluctuations in the motion of particles are increased and granular temperature grows. This behavior is physically coherent reinforcing the correctness of the predictions of normal axial stresses, which in fact determine the granular temperature.
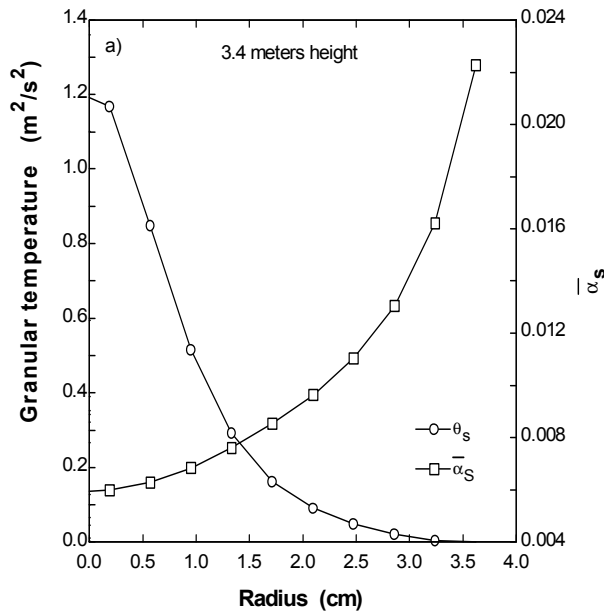
Figure 7. Time averaged radial profiles of granular temperature and solid fraction in the cloumn's left side 3.4 m above entrance.

Neri & Gidaspow (2000) determined granular temperature by solving a granular energy equation coupled with the momentum equations. Neri & Gidaspow's plots of granular temperature against time averaged solids fraction are qualitatively similar to those obtained in this work, which are shown in Figure 8. Still, both the results are similar to the figures of Gidaspow & Huilin (1998), who determined granular temperature through experiment. It seems that the same qualitative correct results of granular temperature are found by either solving a granular energy equation or deriving Reynolds stresses. This is clearly a matter requiring further thought.
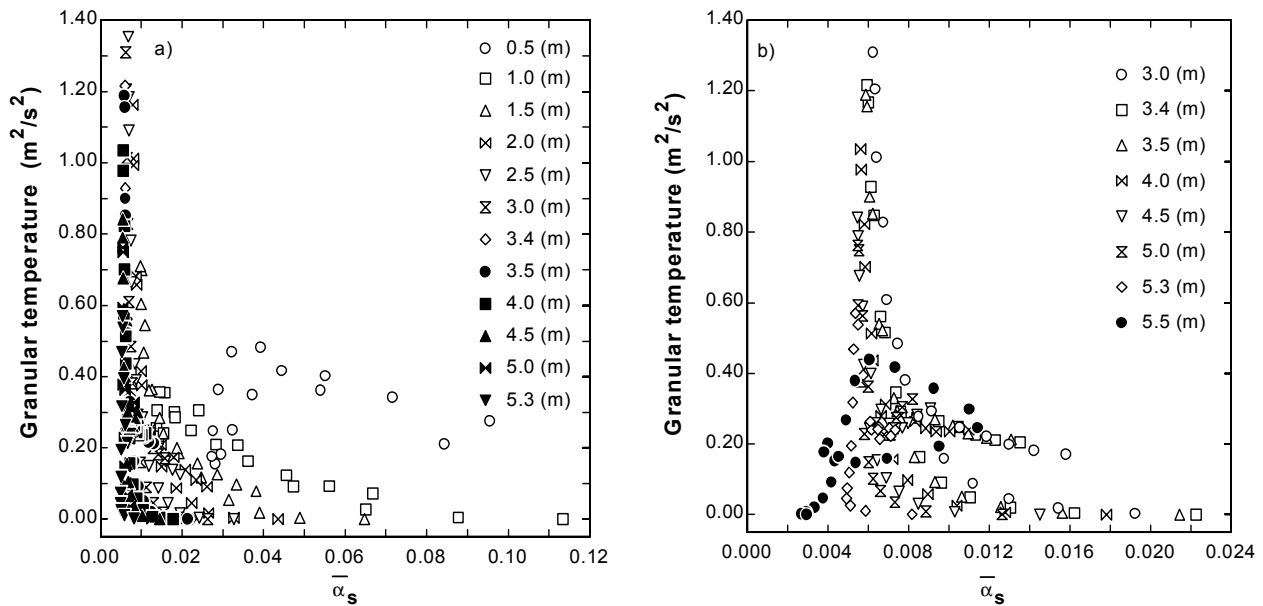

Figure 8. Granular temperature determined from Equation 4 against time averaged solids fraction in various different sections of the column.

Figure 9 presents results for the dynamic viscosity of the solid phase determined as a function of the granular temperature obtained from Reynolds stresses (Equation 5). Despite the agreement in terms of qualitative behavior, the quantitative results significantly differ of those obtained for granular temperature derived from granular energy conservation. The average value of solids viscosity determined through Equation 5 resulted about 7.5×10^{-5} kg/(ms), several orders higher than the experimental average of 0.509 kg/(ms) used in this work. The discrepancy is not quite a surprise since the simulation was performed imposing a constant solid viscosity in each computational cell, disregarding its obvious relation to the solids fraction which changes dramatically in time and all over the computational domain.
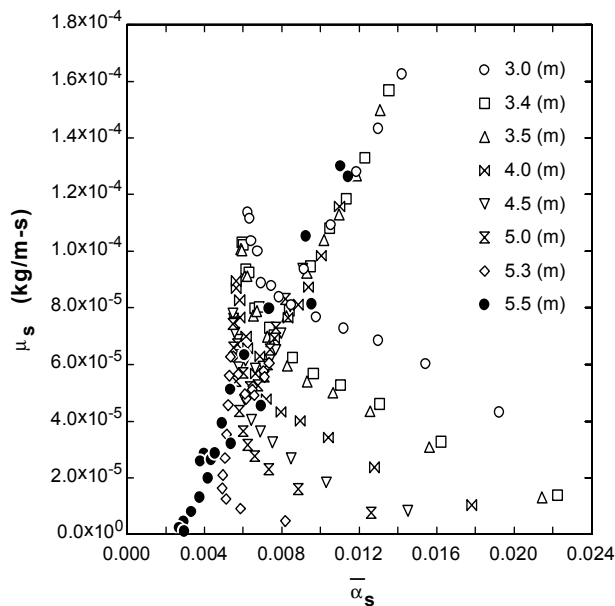
Figure 9. Dynamic viscosity of the solid phase (Equation 5) against time averaged solids fraction.

5. Conclusions

The simulations showed that the traditional two fluids model adequately catches the mean macroscopic features of a gas-solid flow in the riser of a CFB. This includes the well known low frequency flow oscillations, annular plug flow pattern, and clustering. Turbulent parameters were determined assuming that a DNS approach was actually followed for the solid phase. Despite quantitative disagreement regarding literature results, both simulated and experimental, the predictions showed a good qualitative behavior. The behavior of normal axial Reynolds stresses was different from that observed in gas-liquid and gas-liquid-solid systems. A dense downflow of solids was observed at the walls leaving a dispersed upflow plug around the axis. The maximum normal axial Reynolds stresses occurred around the axis, and caused the granular temperatures to be higher at this region. Contrary to the bubble columns, normal axial Reynolds stresses resulted orders of magnitude higher than normal radial and shear Reynolds stresses. In this work granular temperature was derived from continuum hydrodynamic data so that such a procedure could be analyzed. Comparisons of granular temperature were performed against both experiment and granular energy predictions. In spite of the favorable qualitative comparisons, it must be pointed out that such a procedure is possibly inadequate and inconsistent. The solution of a granular energy conservative equation is strongly recommended.

6. Acknowledgements

7. References

Bagnol, R.A. (1954), "Experiments on a Gravity-Free Dispersion of Large Solid Spheres in a Newtonian Fluid under Shear", Proceedings of Royal Society, Vol. A225, p.49-63.
Cabezas-Gómez, L., Milioli, F.E. (2002), "Numerical Study on the Influence of Various Physical Parameters over the Gas-solid Two-phase Flow in the 2D Riser of a Circulating Fluidized Bed", Powder Technology (accepted for publishing PTEC 4733).
Cabezas-Gómez, L., Milioli, F. E. (2001), "Gas-solids two-phases flow in the riser of circulating fluidized bed: mathematical modelling and numerical simulation", Journal of the Brazilian Society of Mechanical Sciences, Vol. XXIII, n.2, p.179-200.
Chapman, S., Cowling, T.G. (1970), The mathematical theory of non-uniform gases, 3rd Ed., Cambridge University Press, Cambridge, U.K.
Ding, J., Gidaspow, D. (1990), "A bubbling model using kinetic theory of granular flow", AIChE Journal, Vol. 36, n.4, p.523-538.
Enwald, H., Peirano, E., Almstedt, A.-E. (1996), "Eulerian two-phase flow theory applied to fluidization", International Journal of Multiphase Flow, Vol. 22, p.21-66, Supplement.
Ergun, S. (1952), "Fluid flow through packed columns", Chemical Engineering Progress, Vol48, n.2, p.89-94.
Gidaspow, D. (2000), "Computation and measurement of structure and turbulence in risers and bubbling beds", Multiphase Fluid Dynamics Research Consortium, Semi-Annual Meeting and Review, Apr. 12-14, Albuquerque, New Mexico.

Gidaspow, D. (1994), Multiphase flow and fluidization: continuum and kinetic theory descriptions, Academic Press Inc., Bostom.

Gidaspow, D., Huilin, H. L. (1998), "Equation of state and radial distribution functions of FCC particles in a CFB", AIChE Journal, Vol. 44, n.2, p.279-293.

Jayaswal, U. (1991), Hydrodynamics of multiphase flows: separation, dissemination and fluidization, Illinois Institute of Technology, Chicago, (Ph.D. Thesis).

Luo, K. M. (1987), Dilute, Dense-Phase and Maximum Solids-Gas Transport, Illinois Institute of Technology, Chicago, (Ph.D. Thesis).

Matonis, D., Gidaspow, D., Bahary, M. (2001), "CFD simulation of flow and turbulence in a slurry bubble column", AIChE Journal, Vol. 48, n.7, p.1413-1429.

Mudde R. F., Lee D. J., Reese J., Fan L.-S. (1997), "Role of coherent structures on Reynolds stresses in a 2-D bubble column", AICHE Journal, Vol. 43, n.4, p.913-926.

Neri, A., Gidaspow, D. (2000), "Riser hydrodynamic: simulation using kinetic theory", AIChE Journal, Vol. 46, n.1, p.52-67.

Pan, Y., Dudukovic, M. P., Chang, M. (2000), "Numerical investigation of gas-driven flow in 2-D bubble columns", AIChE Journal, Vol. 46, n.3, p.434-449.

Peirano, E., Leckner, B. (1998), "Fundamentals of turbulent gas-solid flows applied to circulating fluidized bed combustion", Progress in Energy and Combustion Science, Vol. 24, n.4, p.259-296.

Sinclair, J. L. (1997), Hydrodynamic Modeling. In: GRACE, J. R. et al. Circulating Fluidized Beds, Chapman & Hall. Cap. 5, p.149-180.

Sundaresan, S. (2000), "Modeling the hydrodynamics of multiphase flow reactors: Current status and challenges", AIChE Journal, Vol. 46, n.6, p.1102-1105.

Tennekes, H., Lumley, J. L. (1977), A first course in turbulence, MIT Press, Cambridge, MA.

Tsuo, Y. P., Gidaspow, D. (1990), "Computation of flow patterns in circulating fluidized beds", AIChE Journal, Vol. 36, n.6, p.885-896.

Wen, C. Y., Yu, Y. H. (1966), "Mechanics of fluidization", Chemical Engineering Progress Symposium Series, Vol 62, n.62, p.100-111.

8. Copyright Notice